

# Surface Plasmon Resonance Tunability in Au-VO<sub>2</sub> Thermo-chromic Nano-composites

M. Maaza<sup>1</sup>, O. Nemraoui<sup>2</sup>, C. Sella<sup>3</sup> and A.C. Beye<sup>4</sup>

<sup>1</sup> Nanosciences Laboratories, Materials Research Group, iThemba LABS, PO Box 722, Somerset West 7129, South Africa. E-mail: maaza@tlabs.ac.za

<sup>2</sup> Physics Dept., Rand Afrikaans University, Auckland Park, PO Box 392, Johannesburg, South Africa.

<sup>3</sup> Laboratoire d'Optique des Solides, Universite Pierre-Marie Curie, Paris VI, Jussieu, Paris Cedex 0005, France.

<sup>4</sup> Princeton Materials Institute, Princeton University, Princeton, NJ 08544, USA.

## Abstract

**A new type of photo-active nano-composite material appropriate for Ultra-fast Nonlinear Optical  $\chi^{(3)}(\omega)$  applications has been synthesized and optically characterized. Compared to standard noble metal particles- oxide nano-composites exhibiting a superior effective  $\chi^{(3)}(\omega)$  due to the enhancement of the local electric field, these Au-VO<sub>2</sub> nano-composites display an additional reversibly tunable surface plasmon frequency under external temperature stimuli. Such a smart plasmon tunability is correlated to the Mott's type semiconducting/metallic 1st order transition of the host VO<sub>2</sub> matrix. The nano-gold surface plasmon wavelength shifts reversibly from 645 nm to 598nm when the Au-VO<sub>2</sub> nano-composites temperature varies from 25°C to 120°C.**

## 1 Introduction

Noble metal nanoparticles are well known for their strong interactions with light through the resonant excitations of the collective oscillations of the conduction electrons, the so-called surface plasmon resonances (1-2). The typical surface plasmon resonance of gold nano-particles, specifically, manifests itself through the effective optical absorption peak in the UV/VIS spectrum at about 520nm. Any changes in the environment of the gold nano-particles, the nature of the surface binding, or the degree of interaction between gold nano-particles, will alter this feature. These changes form the basis of numerous spectroscopy probing methods. Recently, within the expansion of the multidisciplinary field of Nanosciences, this surface plasmon resonance effect, involving noble metals, is frequently used for biosensing to monitor binding and changes in biological molecules (3-4) and to improve immunolabeling (5). Likewise, it is used for ultra-low doses gas sensing and bio-hazardous gases identification (6) as well as high-sensitivity electrochemical studies (7). In the standard Kretschmann geometry, this surface plasmon resonance is used to monitor with a high accuracy the optical parameters of Langmuir-Blodgett synthesized thin films (8-9). Similarly, this superior sensitivity related to Kretschmann geometry is used in enhanced Raman spectroscopy in nano-sized particles (10). Alike, generation of discrete surface plasmon modes based nanostructures allowed to synthesize tunable narrow band infrared emitters (11). Finally, through the forces in optical near fields coupled to surface plasmon resonance of nano-gold, the possibility of orientational imaging of single molecules was indeed demonstrated (12-13). Besides this well established linear optical phenomenon of surface plasmon resonance with gold nano-particles, there are additional related nonlinear optical potentialities. Lately, it has been shown that the exploitation of the optical surface 2nd harmonic generation at the vicinity of the plasmon resonance could be extended as a very sensitive probing method of nano-gold in diverse environments (14). More accurately, it has been demonstrated that this nonlinear optical technique is very sensitive to the surface plasmon excitation, the second harmonic signal being resonantly enhanced when the harmonic wavelength is tuned in the vicinity of the plasmon resonance (15).

In regard of 3rd order nonlinear optical NLO properties, at the vicinity of the plasmon resonance, gold based nano-composites, Figure 1, exhibit an ultra-fast enhanced NLO  $\chi^{(3)}$  values coupled with an ultra-fast response in the femto-second regime (10). In actual fact, such a strong enhancement of the 3rd nonlinear optical susceptibility  $\chi^{(3)}(\omega)$  was found to be induced by the local electric field within the metallic nano-particles as alluded to previously by Ricard et al (16-19). Since, these metallic-insulator nano-composites in general are macroscopically isotropic, their 2nd NLO is negligible while their nonlinear response is mainly of 3rd order. In juxtaposition with the induced dipole polarization of the two-phase medium, Figure 1, the local electric field  $E_{loc}$  within the metallic

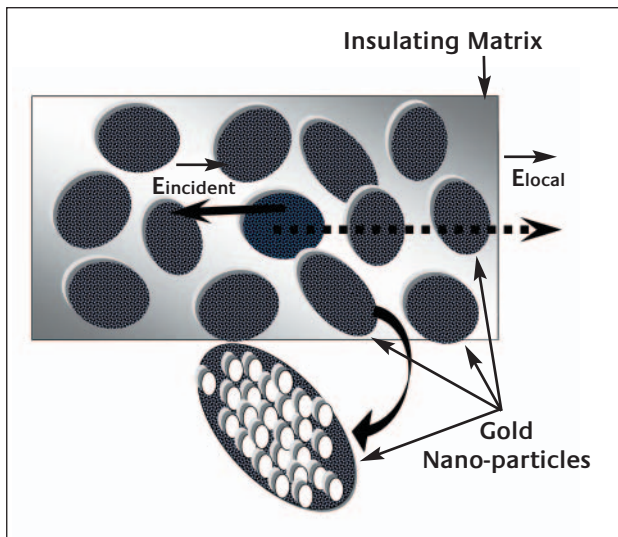


**Figure 1**  
Configuration of a typical metal-insulator nano-composite

nano-particles is related to the exciting electromagnetic field  $E_{inc}$  through the form factor  $f(\omega)$ . On the assumption that the nano-particles are spherically shaped and that they occupy a small volume fraction,  $p \ll 1$ , the effective frequency dependent 3rd NLO susceptibility  $\chi^{(3)}(\omega)$  of such a nano-composite has been found to be:

$$\chi^{(3)effective}(\omega) = p \cdot f^2(\omega) |f(\omega)|^2 \chi^{(3)metal}(\omega) \quad (1)$$

$$f(\omega) = 3 \epsilon_d(\omega) / (\epsilon_{metal}(\omega) + 2 \epsilon_d(\omega)) \quad (2)$$

**Table 1**

Typical values, in esu units, of effective  $\chi^{(3)}$  of Gold-based inorganic/organic nanocomposites from recent literature in both nanosec, picosec and femtosec regimes. 1-Co-Sput.: Co-Sputtering, 2- Colloi.: Colloidal, 3- Poly.: Polymer, 4- Acet.: Acetone, 5- Diel.: Host Dielectric matrix, 6- Synth.: Method of synthesis, 7-  $\langle \phi/2 \rangle$ : average radius of nano-gold particles in nm, 8-  $\lambda_{pr}$ : Plasmon resonance frequency, 9-  $\lambda_e$ : Excitation laser frequency, 10-  $\tau_{laser}$ : pulse duration of the excitation laser beam, 11-  $\chi_{eff}$ : Experimental deduced 3rd NLO

Diel.	Synth.	$\langle \phi/2 \rangle$ (nm)	% Au	$\lambda_{pr}$ (nm)	$\lambda_e$ (nm)	$\chi_{eff}$ (esu)	$\tau_{laser}$	Ref.
SiO <sub>2</sub>	Co-Sput.	3.5-13	2-3	528 540	480 560	1 10 <sup>-7</sup>	20ns	[20]
SiO <sub>2</sub>	ion-impl.	5-30	4-7 10 <sup>-2</sup>	-	532	2 10 <sup>-9</sup>	35ps	[21]
SiO <sub>2</sub>	doped Glasses	1.4-15	1.10 <sup>-5</sup>	530 527	532	8 10 <sup>-14</sup> 5.5 10 <sup>-11</sup>	25ps 5ps	[22]
SiO <sub>2</sub>	Co-Sput.	3-80	5-63	520 545	532	2 10 <sup>-9</sup> 2.5 10 <sup>-6</sup>	70ps	[23]
SiO <sub>2</sub>	Co-Sput.	3	13-19	539	532	-2.11 10 <sup>-6</sup>	7ns	[24]
SiO <sub>2</sub>	ion-impl.	2.9	7.9	525	532	1.2 10 <sup>-7</sup>	7ns	[25]
SiO <sub>2</sub>	ion-impl.	1.5-3	1	505	532	1.5 10 <sup>-8</sup>	7ns	[26]
SiO <sub>2</sub>	ion-impl.	5-25	5		532 591	1.86 10 <sup>-11</sup> 2.93 10 <sup>-6</sup>	6ps	[27]
Al <sub>2</sub> O <sub>3</sub>	Co-Sput.	10-250	25-60	545 590	532	1.2 10 <sup>-6</sup>	70ps	[28]
TiO <sub>2</sub>	Co-Sput.	10-250	15-60	630 670	532 670	8 10 <sup>-6</sup> 6 10 <sup>-7</sup>	20fs	[29]
Colloi.	Hydrosol	10	510 <sup>-6</sup>		530	1.5 10 <sup>-8</sup>	28ps	[30]
Poly.	Organo.	24	7.210 <sup>-3</sup>	550		1 10 <sup>-8</sup>	20ns	[31]
Acet.		5-40	1.10 <sup>-6</sup>	535	516 522	-7 10 <sup>-12</sup> -4.2 10 <sup>-12</sup>	500ps	[32]

$\epsilon_{metal}(\omega)$  and  $\epsilon_d(\omega)$  are the complex dielectric constants of the metallic nano-particles and the dielectric host matrix respectively. When considering the frequency dependence of the factor  $f(\omega)$ , it may be noted that  $f(\omega)$  becomes colossal at the vicinity of the plasmon resonance frequency  $\omega_p$ , the frequency for which the denominator of equation (2) tends to 0:  $(\epsilon_m(\omega_p) + 2\epsilon_d(\omega_p)) \approx 0$ . Therefore, at this optical frequency  $\omega_p$ ,  $\chi^{(3)eff}(\omega)$  of the nano-composite can overtake giant values as a result of the enhancement reinforced by the power 4 of the form factor  $f(\omega)$  compared to those found in classical bulk materials. Degenerate four-wave mixing as well as Z-scan measurements in Ag and Au as well as Cu based nano-composites consistently revealed the colossal third order nonlinear optical susceptibilities  $\chi^{(3)eff}(\omega)$  of about 10<sup>-7</sup>–10<sup>-9</sup> esu in the vicinity of the surface plasmon resonance, with response times of the order of picoseconds, Table 1, (20-32). This enhanced  $\chi^{(3)eff}(\omega)$  offered by this new class of nano-composites is opening new perspectives in emerging nanophotonics sector. In this sense, these emerging NLO nanophotonics would be further valuable if they could additionally exhibit a frequency tunability of their  $\chi^{(3)eff}(\omega)$ . Such a frequency tunability perspective could be envisaged if one can tune the surface plasmon frequency " $\omega_p$ " by an external stimulus exclusively. There are a number of mechanisms which allow such a tunability but in a limited degree of freedom except, a priori, one procedure which is the cornerstone of this contribution.

The collective oscillation plasmon frequency,  $\omega_p$ , of metallic nano-particles embedded in a host matrix, is given by:

$$\omega_p^2 = (ne^2/\epsilon_0 m_{\text{eff}})/(1 + 2\epsilon_d(\omega)) \quad (3)$$

As one can anticipate, this collective oscillation of electron density could, within the metallic nano-particles, be tuned by varying either the electron density “n” or the effective electronic mass,  $m_{\text{eff}}$ , (33). In addition, it can be varied by affecting the shape symmetry of the nano-particles themselves inducing both transversal and longitudinal modes (34). Furthermore, as indicated by equation (3), since  $\omega_p$  is related to the dielectric function of the different materials in the nano-composite, it can be varied by changing the host matrix optical constants,  $\epsilon_d$ . This is illustrated by the experimental literature reported on both Ag and Au nano-particles embedded in different host matrices such as  $\text{Fe}_2\text{O}_3$ ,  $\text{SiO}_2$ ,  $\text{TiO}_2$  and  $\text{Nb}_2\text{O}_5$  (35). Higher is the refractive index of the host matrix “ $n(\text{Fe}_2\text{O}_3)= 2.94$ ,  $n(\text{TiO}_2)= 2.67$ ,  $n(\text{Nb}_2\text{O}_5)= 2.23$  and  $n(\text{SiO}_2)= 1.76$ ” larger is the red-shift. In this particular case, the  $\omega_p$  variation is reasonably sizeable: from 2.4 eV down to 1.7 eV for nano-gold. Naturally, such a consequential variation of  $\omega_p$ , entails a change of the host insulating matrix which is not a very practical way in nano-photonics requiring an  $\omega_p$  tunability, and therefore a possible externally driven  $\chi^{(3)\text{eff}}(\omega)$  tunability. One should mention that it has been showed experimentally that  $\omega_p$  can be thermally varied but not in a controllable approach. This thermal variation takes place in semimetals as exhibited experimentally by the surface excitation of graphite (36). This temperature variation  $\omega_p(T)$  has been attributed to the excitation of  $\pi$ - band plasmon polarized with E parallel to the c-axis. Likewise, one should mention the tunability of the plasmon resonance frequency in core-shell gold-insulating particles “nano-scaled gold as a shell” (37). In the case of  $\text{SiO}_2$  core,  $\approx 100$  nm in  $\langle\phi\rangle$ , coated with a nano-sized gold shell with thickness varying from 5 to 25 nm, the plasmon resonance wavelength varies from  $\approx 1027$  nm to  $\approx 730$  nm (37). Even if the tunability option is achievable, yet again, once the shell thickness/core size coupled value is fixed, the plasmon resonance cannot be tuned.

As pointed out previously, the cornerstone of this contribution is to present a novel method to thermally tune the surface plasmon frequency  $\omega_p$  and therefore  $\chi^{(3)\text{eff}}$  in a controllable manner for potential nonlinear applications of the considered Au based nano-composite without changing the insulating initial host matrix. This new innovative approach combines the advantages of the two above mentioned  $\omega_p$  tunability; namely the variation of the refractive index of the host matrix in addition to the  $\omega_p(T)$  thermal variation as in semi-metals. In general, the intrinsic optical properties of a material are determined by three physical processes: free electrons, lattice vibrations, and electronic transitions. The dominant physical process depends on the nature of the material. All materials have contributions to the complex index of refraction from electronic transitions. Metals and semiconductors are additionally influenced by free carriers

effects. The strength of this effect depends on the carrier concentration; thus, it is very important for metals. The temperature, T, and frequency,  $\omega$ , dependence of the real part of the refractive index,  $n(T, \omega)$ , is determined by the dominant physical processes previously mentioned. The temperature and frequency dependence of the imaginary part of the index of refraction,  $k(T, \omega)$ , (Index of extinction), is more involved and requires consideration of not only the dominant physical processes but also higher order processes, impurities and defects. The temperature dependence of the refractive index  $n^*(T, \omega) = n(T, \omega) - j k(T, \omega)$  could be estimated using the Lorentz-Lorentz formula (38):

$$[n^2(T, \omega) - 1] / [n^2(T, \omega) + 2] = \rho(T) \alpha_p(\rho, T) / 3 \epsilon_0 \quad (4)$$

where  $\rho$ ,  $\rho=N/V$ , is the number density of oscillators per unit volume, N is the number of oscillators per unit volume and  $\alpha_p$  is the polarizability. The derivative of the refractive index with respect to “T” becomes (39):

$$2n \epsilon_0 dn/dT = - (n^2+2).(n^2-1) \{ \alpha_p.[1-(V/\alpha_p)] (\partial\alpha_p/\partial V)_T + [(\partial\alpha_p/\partial T)_V]/3\alpha_p \} \quad (5)$$

The first term depends on changes in volume with respect to temperature. Thermal expansion is the dominant contributor. The second term represents the temperature changes in the polarizability. Many optical materials, such as the alkali halides and fluorides, have negative values for  $dn/dT$  in the VIS and IR spectral regions. Thus, for these materials, volume expansion dominates over polarizability temperature dependence.

In this contribution, a specific host material for gold nano-particles, with a temperature driven refractive index has been considered. This host matrix consisting of Vanadium Dioxide  $\text{VO}_2$ , undergoes a semiconducting-metallic transition when the temperature is raised above the critical value of  $T_c \approx 68^\circ\text{C}$ , with a jump-like change of the electric conductivity by several orders of magnitude. This thermally driven first order phase transition of the host  $\text{VO}_2$  concurs with a crystallographic phase transition from monoclinic to tetragonal and is accompanied by a strong variation in electric, magnetic and specific heat properties (38-43). This semiconductor-metal phase transition is followed naturally by a sharp optical transition and therefore a variation of the optical constants: the real and imaginary parts of the refractive index  $n^*(T) = n(T) + j k(T)$ . This change  $n^*(T)$  is, specifically, pronounced in the Infrared spectral region. This latter has been investigated comprehensively by Verleur et al and Barker et al (44). One should mention that recent femtosecond laser investigations have been carried out to study the dynamic response of the  $\text{VO}_2$  refractive index as well to measure the structural transition duration which was found to occur within  $\approx 500$  fs (45-46). Such an ultrafast change in complex refractive index with temperature should enable ultra-fast optical switching devices based on  $\text{VO}_2$  (47).

In this communication, the externally controllable tunability of the nano-gold surface plasmon frequency resonance by

temperature in the range of 25-120°C in non percolated Au-VO<sub>2</sub> nano-composites is demonstrated.

## 2 Experiments and Results

XeCl pulsed laser ablation non percolated Au-VO<sub>2</sub> nano-composites with a thickness ranging from 135±5 to ≈170±5 nm have been deposited on to Corning glass substrates. The volume concentration of nano-gold, ≈29%, was kept below the percolation threshold to ensure a homogeneous colloidal-like distribution of the nano-sized gold particles within the host VO<sub>2</sub> matrix. The different Au-VO<sub>2</sub> nano-structures were subjected to Atomic Force Microscopy, AFM, X-Ray Diffraction, XRD, and VIS-NIR optical measurements. These latter measurements were carried out within the range of 25-100°C.

Figure 2 shows the room temperature atomic force microscopy surface profile of a typical pulsed laser deposited sample with nano-gold average diameter of about  $\langle\phi\rangle \approx 12.7\text{nm}$  and labeled as Au- $\langle\phi\rangle=12.7\text{nm}$ -VO<sub>2</sub>, thickness ≈160 ±3 nm. Generally, all deposited films consist of very compact grains. This expected dense structure is a characteristic of films deposited by laser ablation (50). It is explained, generally, by the fact that the ablated clusters from the Vanadium dioxide target component is most likely ejected in the form of fairly large molecular clusters. The coalescence of these molecular clusters on the substrate could be favoured by the flash radiative heating because the rates of heating and cooling are faster than what phase separation cannot occur in the bulk material. Based on such an hypothesis and compared to VO<sub>2</sub> nano-structures synthesized by other vacuum processing methods, one can indeed explain the high surface roughness observed on all current PLD synthesized nano-structures. The surface topography of the Au- $\langle\phi\rangle=12.7\text{nm}$ -VO<sub>2</sub>

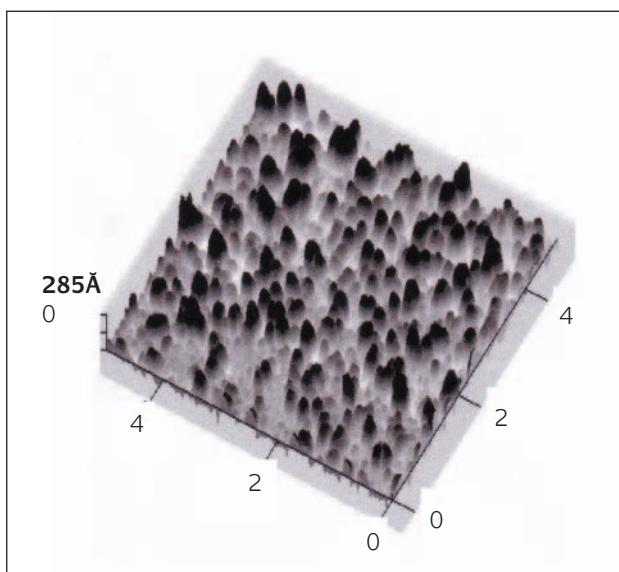


**Figure 2**  
Atomic force microscopy topography of “Au- $\langle\phi\rangle \approx 12.7\text{nm}$ -VO<sub>2</sub> nano-composite/ Corning glass sample, “thickness ≈ 160 ±3 nm”

nanocomposite presents a relatively rough profile. While the average value of the root mean square roughness is about 6.1nm, the mean height distribution is of the order of 29.7 nm. This latter high value is correlated to the numerous conical-like islands observed on the surface as shown in Figure 2. These conical-like topography with approximately 193.2 nm in base and 27.9 nm in height within the surface is related to the columnar growth mechanism in the transversal direction well established in the case of this type of nano-composites synthesized by sputtering and laser ablation. The XRD investigations with CuK $\alpha$  radiations of 1.54 Å, showed that the VO<sub>2</sub> host matrix presents an effective (111) crystalline orientation (51). Likewise, the large intensity of a Bragg peak located at  $2\theta \approx 38.22 \pm 0.08$  deg indicates the presence of crystalline Au nano-particles with a possible cubic structure of (111) orientation. The average size  $\langle\phi\rangle$  deduced from XRD linewidth using Debye-Scherrer approximation was found to be of the order of 12.7 nm.

The optical measurements were carried out with a Cary-type spectrophotometer in the wavelength interval of 290–3000 nm in normal incidence configuration. To substantiate the thermal tunability of the surface plasmon frequency in the investigated Au-VO<sub>2</sub> nano-composites, the optical measurements were made on the samples held in an optical fixture housed in an evacuated system with an in-situ heater for temperature cycling. The optical transmission measurements were performed in a reversible manner with the temperature cycling from 25°C to 120°C and vice-versa. As the experimental optical trends of the different Au-VO<sub>2</sub> nano-composites were found to be quite similar, we report only the optical transmission measurements corresponding to the Au- $\langle\phi\rangle=12.7\text{nm}$ -VO<sub>2</sub> nano-composite on Corning glass sample.

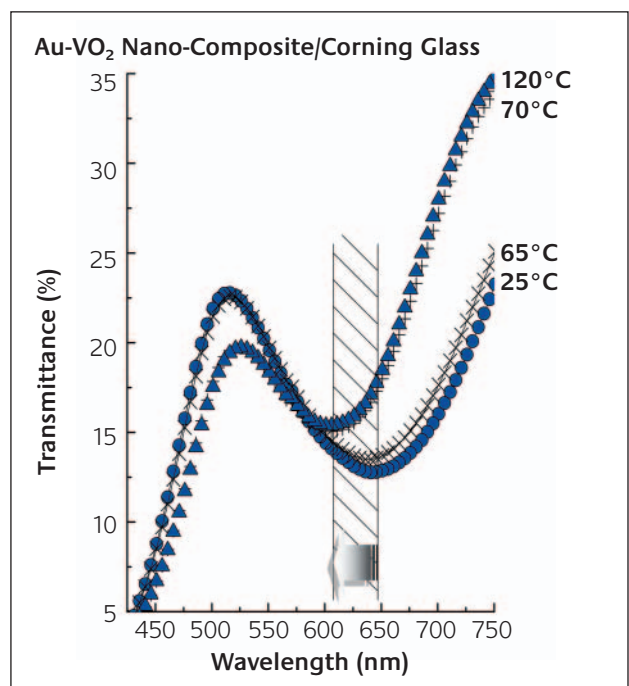


**Figure 3**  
Optical transmission of Au- $\langle\phi\rangle \approx 12.7\text{nm}$ -VO<sub>2</sub> nano-composite/Corning glass sample below and above the transition temperature  $T_c \approx 68^\circ\text{C}$

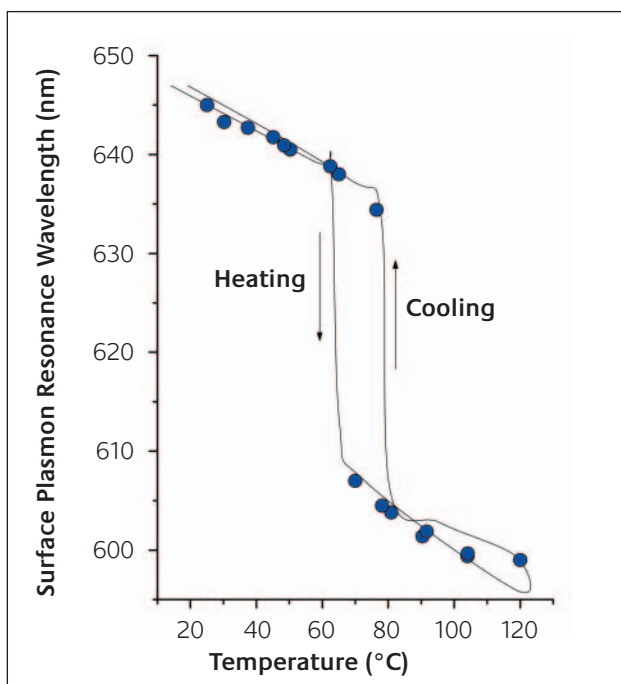


**Figure 4**  
 Representative temperature evolution of the nano-gold surface plasmon wavelength below and above  $T_c \approx 68^\circ\text{C}$ . of the  $\text{Au}_{\langle\phi\rangle} \approx 12.7 \text{ nm} - \text{VO}_2$  nano-composite/Corning glass sample. The line is an eye guide

Even if the modulation in the optical transmission is very large in the near infrared as expected, we limited the study to the spectral range of 425-750 nm in order to focus on the shift of the nano-gold surface plasmon wavelength, if any. Figure 3 displays the corresponding optical transmission versus the wavelength of the incident beam for 4 representative heating temperatures, below 25 and 65 °C and above 70 and 120 °C the critical temperature  $T_c$  of 68 °C. While the nano-gold surface plasmon wavelength is about 648 nm below  $T_c$ , it shifts obviously to 603 nm above  $T_c$  towards the blue. This nano-gold surface plasmon shift is consequential variation of  $\approx 45$  nm and sizeable enough and confirms the option of tunability of  $\omega_p$  via an external temperature stimuli. This thermally driven variation of  $\omega_p(T)$  confirms the valuable purpose of this communication. As mentioned previously, the spectral position of the plasmon frequency depend in fact not only on the relative refractive index of the hosting matrix but also on the size of the metallic nano-particles. According to Mie theory and even more advanced theoretical models such as the effective medium model, smaller is the metallic nano-particles, blue is the shift of the plasmon frequency. This is evidenced clearly in some elegant experiments using nano or/and femtosec regimes of laser induced size reduction of noble metal particles (52-54). Figure 4 reports the experimental variation of the nano-gold surface plasmon wavelength versus temperature. As shown, it decreases quasi-linearly with the following slopes of  $-0.18 \text{ nm}/^\circ\text{C}$  and  $-0.17 \text{ nm}/^\circ\text{C}$  below and above  $T_c$  respectively while it falls sharply around  $T_c$ . Such an expected abrupt variation at the vicinity of  $T_c$  is, indeed, associated with the first order transition nature of the host

matrix  $\text{VO}_2$  with temperature. Moreover the curve displays the anticipated hysteresis with a bandwidth of the order of 8 °C. This hysteresis corresponding to the heating-cooling phenomenon of the host  $\text{VO}_2$  matrix is related to the degree of crystallinity of the host matrix (55-57). The sharpness of the temperature variation of the surface plasmon wavelength in the vicinity of  $T_c$  is due to the fact that the host  $\text{VO}_2$  matrix is highly crystalline as shown by the principal  $\text{VO}_2$  narrow (111) Bragg peak (51). Such a high epitaxial growth extent is a characteristic of the laser deposition in vacuum procedure (57). Hence, to smooth out the abrupt temperature variation in the vicinity of  $T_c$ , two options could be considered. The first involves minimizing the crystallinity of the host  $\text{VO}_2$  matrix while the second involves tungsten doping of the same matrix (50, 55-57). There is an alternative option which involves using a combination of  $\text{Ti}_2\text{O}_3$  with the  $\text{VO}_2$  host matrix. Effectively, a smooth nonmetallic-metallic transition with temperature prevails in  $\text{Ti}_2\text{O}_3$  (56, 58-59) in the range of 177 °C-377 °C in particular.

As depicted by figure 3, the optical transmission in the visible spectral part is low; at 525 nm approximately, its value is about 22.5% and 19.7% below and above  $T_c$ . Therefore, such an Au- $\text{VO}_2$  nanophotonic device would be impractical in its current form for tunable third order frequency  $\chi^{(3)\text{eff}}(\omega)$  generation. Indubitably, one should enhance the optical visible transmission by a genuine approach. As substantiated experimentally by Khan et al (60), fluorine doping of the order of  $6.20 \pm 0.60$  %atomic of the  $\text{VO}_2$ -F host matrix increases significantly the VIS transmission. Naturally, such an "F" doping should be coupled with a thickness optimization as well as the Au- $\text{VO}_2$  nano-composite. Such an optimization is currently in progress in our labs.

### 3 Conclusion

Surface plasmon tunability has been demonstrated in Au- $\text{VO}_2$  nano-composites. Such a surface plasmon tunability is induced thermally and reversibly in a controllable way, within the range of 25-120 °C. Even if the nano-gold surface plasmon variation is not dramatic " variation from 548 nm to 600 nm", it is substantial. For possible  $\chi^{(3)}$  NLO applications, the VIS optical transmission of these Au- $\text{VO}_2$  nano-composites should be increased by fluorine doping of the host oxide  $\text{VO}_2$  and optimization of the nano-composite thickness. New nano-gold based nano-photonics will be explored. These latter consist of Au- $\text{V}_3\text{O}_5$  and Au- $\text{NbO}_2$  nano-composites. Both  $\text{V}_3\text{O}_5$  and  $\text{NbO}_2$  exhibit, as the considered  $\text{VO}_2$  host matrix, a semiconducting-metallic 1st order transition at 147 and 797 °C respectively.

### 4 Acknowledgements

This research program was financially supported by the International Liaison Office of the National Research Foundation, the French Centre National pour la Recherche

Scientifique. We are grateful to the Rand Afrikaans Universiteit and the University of the Witwatersrand Research Council for their technical and financial supports respectively. Likewise, we are grateful to Mrs. A.M. DAWE from the University of the Witwatersrand for her XRD technical assistance. We are indebted to the members of the National Laser Centre for their valuable infrastructure and technical support.

## 5 About the Authors

Dr O. Nemraoui received his PhD from the University of ParisXI in the field of materials sciences. His research is in the field of surface-interface phenomena as well as advanced and multifunctional materials.

Prof. C. Sella is a Professor at University of Paris VI. He is an expert in the field of vacuum technology, thin films and nano-composites synthesis and optical devices.

Prof. A.C. Beye is an expert in materials sciences. He is the founding President of the African Materials Research Society. He is member of the board of directors of the African Laser Centre, Member of the Nelson Mandela – World Bank African Institutes of Science & Technology. He is the initiator of the US NSF-Africa initiative in Materials sciences. His research interests encompass large fields of materials sciences and laser spectroscopy.

Dr. M. Maaza holds a PhD from the University of Paris VI. He was involved extensively in the investigation of surface-Interface phenomena by neutron and X-Rays scattering. His expertise lies within photonics and nano-materials. He is the initiator of the South African Nanotechnology initiative. He is currently the Chairman of the NANOAFNET (NANOsciences AFrican NETwork), an initiative supported by ICTP: UNESCO-AIEA. He is the Vice-President of the French Council of Scientists and Engineers: South African section and a member of the Nobel Abdus Salam International Centre for Theoretical Physics.

## 6 References

- 1 U. Kriebig and M. Vollmer, in *“Optical Properties of Metal Clusters”*, Springer, Berlin, 1995
- 2 D. Feldheim and C. Foss, in *“Metal Nanoparticles: synthesis, Characterization, and Applications”*, Marcel-Dekker: New York, 2001
- 3 K. Aslan, J.R. Lakowicz and C.D. Geddes, *Anal Biochem.* 2004 Jul 1; 330(1), p.145, 2004
- 4 F. Caruso, M.J. Jory, G.W. Bradberry, J.R. Sambles and D.N. Furlong, *J. Appl. Phys.* **83**, 2, p.5, 1998, Hainfeld, J.F. and Furuya, F.R.A.
- 5 J.F. Hainfeld and F.R.A. Furuya, *J. Histochem. Cytochem.* **40**, p.177, 1992
- 6 M.J. Jory, P.S. Cann and J.R. Sambles, *J. Phys. D: Appl. Phys.* **27**, p.169, 1994

- 7 M.J. Jory, G.W. Bradberry, P.S. Cann and J.R. Sambles, *Meas. Sci. Technol.* **6**, p.1193, 1995
- 8 A.V. Nabok, T. Richardson, F. Davis, C.J.M. Stirling, *Langmuir.* **13**, p.3198, 1997
- 9 D.J. Elliot, D.N. Furlong and F. Grieser, *Colloids and Surfaces A.* **155**, p.101, 1999
- 10 V.M. Shalae, *Physics Reports*, Vol. 272, **2-3**, 61, 1996
- 11 I.El Kady, R. Biswas, Y. Ye, M.F. Su, I. Uscasu, M. Pralle, E.A. Johnson, J. Daly and A. Greenwald, *Photonics and Nanostructures.* **1**, p. 69, 2003
- 12 L. Novotny, in *“Near Field Optics and Surface Plasmon Polaritons”*, S. Kawata, Ed., *Topics in Applied Physics.* **81**, p.123, Springer, Berlin, 2000
- 13 B. Sisek, B. Hecht and L. Novotny, *Phys. Rev. Letts.* **85**, p.44782, 2000
- 14 R. Antoine, B.F. Brevet, H.H. Girault, D. Bethell and D.J. Schiffrin, *Chem. Commun.* p.1901, 1997
- 15 R. Antoine, M. Pellarin, B. Palpant, M. Broyer, B. Prevel, P. Galletto, P.F. Brevet and H.H. Girault, *J. Appl. Phys.* **84**, p.4532, 1998
- 16 F. Hache, D. Ricard, C. Flytzanis and U. Kriebig, *Applied Physics A,* **47**, 347, 1988
- 17 D. Ricard, Ph. Roussignol and C. Flytzanis, *Optics Letters* **10**, 511, 1985
- 18 C. Flytzanis, *Prog. Opt.* **29**, 2539, 1992
- 19 O. Levy, D.J. Bergman and D.G. Stroud, *Phys. Rev. B.* **52**, 3184, 1995
- 20 I. Tanahashi, Y. Manabe, T. Tohda, S. Sasaki and A. Nakamura, *J. Appl. Phys.* **79**, p. 1244, 1996
- 21 R.H. Macgruder, L. Yang, R.F. Haglund, C.W. White, L. Li-Yang, R. Dorsinville and R.R. Alfano, *Appl. Phys. Lett.* **62**, p. 1730, 1993
- 22 F. Hache, D. Ricard, C. Flytzanis and U. Kriebig, *Appl. Phys. A.* **47**, p.347, 1988
- 23 H.B. Liao, R.F. Xiao, J.S. Fu, P. Yu, G.K.L. Wong and P. Sheng, *Appl. Phys. Lett.* **70**, p. 1, 1997
- 24 J. Venturini, PhD Thesis, *University of Paris VI*, 16th December 1999, p.185, 1999
- 25 H.B. Liao, R.F. Xiao, J.S. Fu, P. Yu and G.K.L. Wong, *Appl. Phys. B.* **65**, p. 673, 1997
- 26 H.B. Liao, R.F. Xiao, J.S. Fu, H. Wong, K.S. Wong and G.K.L. Wong, *Appl. Phys. Lett.* **72**, p. 1817, 1998
- 27 K. Fukumi, A. Chayahara, K. Kanado, T. Sakagushi, Y. Horino, M. Miya, J. Hayakawa and M. Satou, *Jap.J. Appl. Phys.* **30**, p.742, 1990
- 28 K. Fukumi, A. Chayahara, K. Kanado, T. Sakagushi, Y. Horino, M. Miya, K. Fuji, J. Hayakawa and M. Satou, *J. Appl. Phys.* **75**, p. 3075, 1994
- 29 D. Ricard, P. Roussignol and C. Flytzanis, *Opt. Lett.* **10**, p. 511, 1985
- 30 L. Yang, D.H. Osborne, R.F. Haglund, R.H. Macgruder, C.W. White, R.A. Zuhr and H. Hosono, *Appl. Phys. A.* **62**, p. 403, 1996
- 31 S. Ogawa, Y. Hayashi, N. Kobayashi, T. Tokizaki and A. Nakamura, *Jpn. J. Appl. Phys.* **33**, p. 331, 1994
- 32 K. Puech and W. Blau, *Opt. Lett.* **20**, p. 1613, 1995
- 33 J.B. Pendry, A.J. Holden, W.J. Stewart and I. Youngs, *Phys. Rev. Lett.* **76**, 25, 4773, 1996
- 34 D.C. Skillman and C.R. Berry, *J. Phys. Chem.* **48**, 7, 3297, 1967
- 35 S. Schiestel, C.M. Cotell, C.A. Carosella, K.S. Grabowski G.K. Hubler, *Nucl. Instrum. Meths. Phys. Res. B.* **127-128**, 566, 1997
- 36 E.T. Jensen, R.E. Palmer, W. Allison and J.F. Annett, *Phys. Rev. Lett.* **66**, 492, 1991

- 37 S.J. Oldenburg, R.D. Averitt, S.L. Westcott and N.J. Halas, *J. Phys. Chem. Lett.* **288**, p. 243, 1998
- 38 A.J. Bosman and E.E. Havinga, *Phys. Rev.* **129**, p. 1593, 1963
- 39 M.E. Thomas and R.I. Joseph, *Infrared Optical Materials, Proc. SPIE* 929, p. 87, 1988
- 40 F.J. Morin, *Phys. Rev. Lett.* **3**, 34, 1959
- 41 G.J. Hill and H.R. Martin, *Phys. Rev. Lett. A.* **27**, 34, 1968
- 42 P.P. Edwards, P.V. Ramakrishnan and C.N.R. Rao, in "Metal-Insulator Transitions Revisited", Eds. P.P. Edwards and C.N.R. Rao, Taylor and Francis, 1995
- 43 N. Mott, in "Metal-Insulator Transitions", Taylor and Francis, London "1997"
- 44 H.W. Verleur, A.S. Barker Jr. and C.N. Berglund, *Phys. Rev.* **17** 2(1), 788, 1968
- 45 M.F. Becker, A.B. Buckman, R.W. Walsler, Th. Lepine, P. George and A. Brun, *Appl. Phys. Lett.* **65** (12), 150, 1996
- 46 A. Cavalleri, C. Toth, C.W. Siders, J.A. Squier, F. Raksi, P. Forget and J.C. Kieffer, *Phys. Rev. Lett.* **87**, 23, p.237, 2001
- 47 R. Lopez, T.E. Haynes, L.A. Boatner, L.C. Feldman and R.F. Haglund Jr., *Phys. Rev. B.* **65**, p. 224113, 2002
- 48 R. Lopez, T.E. Haynes, L.A. Boatner, L.C. Feldman and R.F. Haglund Jr., *Optics Lett.* **27**, p.1327, 2002
- 49 G.I. Petrov, V.V. Yakovlev and J.A. Squier, *Optics Letts.* **27**, Iss. 8, p.655, 2002
- 50 M. Maaza, K. Bouziane, J. Maritz, D.S. McLachlan, R. Swanepoel, J.M. Frogerio and M. Every, *Optical Materials* **15**, 41, 2000
- 51 M. Maaza, O. Nemraoui, C. Sella, G. Hearne, A.C. Beye and B. Baruch-Barak, *To Appear in Optics Communications*, 2004
- 52 A. Takami, H. Kurita and S. Koda, *J. Phys. Chem. B.* **103**, p. 1226, 1999
- 53 K. Kurihara, J. Kizling, P. Stenius and J.H. Fendler, *J. Am. Chem. Soc.* **105**, p. 2574, 1983
- 54 T.S. Ahmadi, S.L. Logunov and M. El-Sayed, *J. Phys. Chem.* **100**, p. 8053, 1996
- 55 A.S. Barker, H.W. Verler and H.J. Gugenheim, *Phys. Rev. Lett.* **17**, p. 1286, 1966
- 56 Gmelin Handbuch, Vol. 16, Section Vanadium Oxides, p. 482
- 57 M. Maaza, C. Sella, O. Nemraoui, N. Renard and Y. Sampeur, *Surface and Coating Technology*. Vol. 97, Iss. 1-3, 1997
- 58 W. Haidinger and D. Gross, *Thin Solid Films* **12**, 433, 1972
- 59 D. Adler, in "Solid. State Physics", Eds. F. Seitz and D. Turnbull and H. Ehrenreich, Academic Press, New York and London, Vol. 21, 1, 1968.
- 60 K.A. Khan, G.A. Niklasson and C.G. Granqvist, *J. Appl. Phys.* **64**(6), 3327, 1988